DOA Estimation for Far-Field Sources in Mixed Signals with Gain-Phase Error Array

Jiaqi Zhen(✉) and Yanchao Li

College of Electronic Engineering, Heilongjiang University, Harbin 150080, China
zhenjiaqi2011@163.com

Abstract. Most of the super-resolution direction finding algorithms often require the accurate array manifold, but the gain-phase of the channels is often inconsistent in practical applications, which will lead to the estimation performance deterioration. Therefore, a new method for direction of arrival (DOA) estimation of far-field sources in mixed far-field and near-field signals with gain-phase error array is presented. First, fast Fourier transformation (FFT) is performed on the received data, then matrix transformation is used for simplifying the spectrum function, at last, DOA of far-field signals can be acquired by finding the roots of corresponding polynomial. There is no need to calibrate the array, simulations have shown that the proposed algorithm is effective.

Keywords: Direction of arrival · Gain-phase error · Far-field signals
Near-field signals · Wideband signals

1 Introduction

Super-resolution direction finding is one of the major researches in array signal, it is extensively applied in radio monitoring [1–3], internet of things [4, 5] and military [6, 7]. Generally speaking, knowing the exact array manifold is the precondition to the estimation, but the gain and the length of the channels are often not the same, which will lead to the estimation performance deterioration, so it is necessary to correct the array.

In general, calibration methods in array signal processing can be classified into using source and self correction. The former are realized by utilizing the assistant signal whose location is known; The latter are usually based on some optimization functions to calculate the directions and perturbation parameters of the array iteratively. Some of these methods have their distinct advantages: Lee [8] proposed a covariance approximation method for near-field direction finding using a uniform linear array, it estimated

J. Zhen—This work was supported by the National Natural Science Foundation of China under Grant Nos. 61501176 and 61505050, University Nursing Program for Young Scholars with Creative Talents in Heilongjiang Province (UNPYSCT-2016017), China Postdoctoral Science Foundation (2014M561381), Heilongjiang Province Postdoctoral Foundation (LBH-Z14178), Heilongjiang Province Natural Science Foundation (F2015015), Outstanding Young Scientist Foundation of Heilongjiang University (JCL201504) and Special Research Funds for the Universities of Heilongjiang Province (HDRCCX-2016Z10).

B. Li et al. (Eds.): ChinaCom 2017, LNICST 237, pp. 41–50, 2018.
https://doi.org/10.1007/978-3-319-78139-6_5

DOA, together with unknown sensor gains and phases in the uncalibrated portion of the array; Liu [9] presented an eigenstructure approach which synchronously obtained the DOA and gain-phase perturbations without joint iteration; Cao and Ye [10] proposed a calibration method for channel gain-phase uncertainty based on fourth-order cumulant technique, it adapts to the background of non-Gaussian signals and Gaussian noise; Han [11] considered the problem of DOA estimation based on a nonuniform linear nested array, which is known to provide $O(N^2)$ degrees of freedom using only N sensors, and the gain-phase errors can also be calculated by different subsequent processing.

In recent years, many experts have developed some DOA estimation algorithms of mixed far-field and near-field sources (FFS and NFS), Liang [12] proposed a two-stage dimensional multiple signal classification (MUSIC) algorithm with cumulant which averted high-dimensional searching and parameters matching; Wang [13] presented a novel localization algorithm for the mixed sources based on the polynomial decomposing method and high-order cumulant technique, but the computation is very complex; In [14], a new mixed NFS and FFS localization algorithm based on sparse signal recovery is addressed, it can provide the improved estimation accuracy comparing with the traditional algorithm. All the methods above only adapt to narrowband signals, but there are rare published literatures of gain-phase uncertainty calibration for mixed wideband signals.

In this paper, a novel method for DOA estimation of far-field sources in mixed far-field and near-field wideband signals in the presence of gain-phase uncertainty is proposed. First, fast Fourier transformation (FFT) is performed on the received data, then matrix transformation is used for simplifying the spectrum function, at last, DOA of far-field signals can be acquired by finding the roots of corresponding polynomial. There is no need to calibrate the array, so as to improve the calculation efficiency on the premise of ensuring some level of precision and it is suitable for wideband coherent signals as well.

2 Array Signal Model

2.1 Ideal Signal Model

It is shown in Fig. 1, there are N_1 far-field linear frequency modulation wideband signals $s_{n_1}(t)(n_1 = 1, 2, \cdots, N_1)$ and N_2 near-field wideband signals $s_{n_2}(t)(n_2 = 1, 2, \cdots, N_2)$ with the same energy arriving at the uniform linear array composed of $2M + 1$ sensors, DOA of these signals are $[\theta_1, \cdots, \theta_{N_1}, \theta_{N_1+1}, \cdots, \theta_N]$, where $N = N_1 + N_2$, the distance of adjacent sensors is d, it is equal to half of the wavelength of the center frequency of these sources, suppose N_1, N_2 is known in advance. The 0-th sensor is deemed to be the reference. The frequency of all signals is limited in $[f_{\text{Low}}, f_{\text{High}}]$, J points of fast Fourier transformation (FFT) are employed for the output of the array, then we can model the signal as

$$\boldsymbol{X}(f_i) = \boldsymbol{A}(f_i, \theta)\boldsymbol{S}(f_i) + \boldsymbol{E}(f_i) \quad (i = 1, 2, \cdots, J) \tag{1}$$

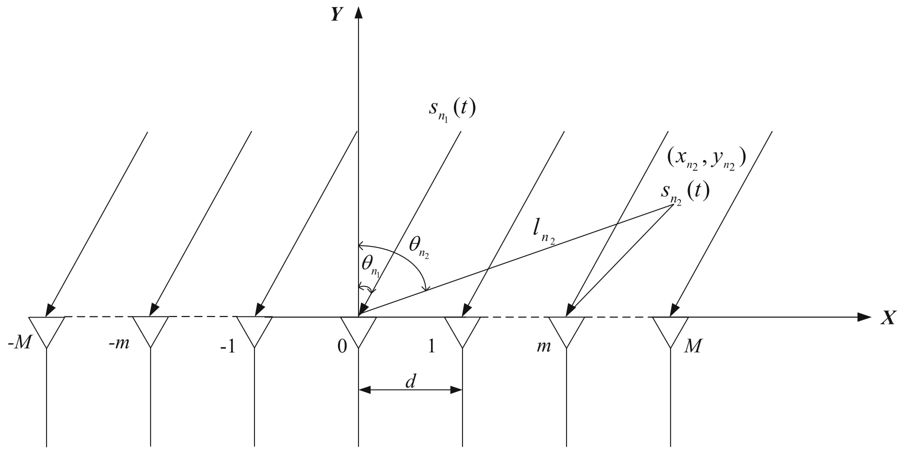

Fig. 1. Array signal model

where $f_{\text{Low}} \leq f_i \leq f_{\text{High}}$, $\boldsymbol{X}(f_i) = [\boldsymbol{X}(f_i,\ 1), \cdots, \boldsymbol{X}(f_i, z), \cdots, \boldsymbol{X}(f_i, Z)]$, Z is the sampling times at every frequency, and

$$\boldsymbol{X}(f_i, z) = [X_{-M}(f_i, z), \cdots, X_{-m}(f_i, z), \cdots, X_0(f_i, z), \cdots, X_m(f_i, z), \cdots, X_M(f_i, z)]^{\mathrm{T}} \quad (2)$$

here $X_m(f_i, z)$ is the z-th sampling data on the m-th sensor at f_i, $\boldsymbol{A}(f_i, \theta)$ is the array manifold at f_i

$$\begin{aligned} \boldsymbol{A}(f_i, \theta) &= [\boldsymbol{a}_{FS}(f_i, \theta_1), \cdots, \boldsymbol{a}_{FS}(f_i, \theta_{n_1}), \cdots, \boldsymbol{a}_{FS}(f_i, \theta_{N_1}), \boldsymbol{a}_{NS}(f_i, \theta_{N_1+1}), \cdots, \boldsymbol{a}_{NS}(f_i, \theta_{n_2}), \cdots, \boldsymbol{a}_{NS}(f_i, \theta_N)] \\ &= [\boldsymbol{A}_{FS}(f_i), \boldsymbol{A}_{NS}(f_i)] \quad (i = 1, 2, \cdots, J) \end{aligned} \quad (3)$$

where $\boldsymbol{A}_{FS}(f_i) = [\boldsymbol{a}_{FS}(f_i, \theta_1), \cdots, \boldsymbol{a}_{FS}(f_i, \theta_{n_1}), \cdots, \boldsymbol{a}_{FS}(f_i, \theta_{N_1})]$ is the array manifold of FFS at f_i ideally, and $\boldsymbol{a}_{FS}(f_i, \theta_{n_1})$ is the corresponding far-field steering vector of $s_{n_1}(t)$; $\boldsymbol{A}_{NS}(f_i) = [\boldsymbol{a}_{NS}(f_i, \theta_{N_1+1}), \cdots, \boldsymbol{a}_{NS}(f_i, \theta_{n_2}), \cdots, \boldsymbol{a}_{NS}(f_i, \theta_N)]$ is the array manifold of NFS at f_i ideally, and $\boldsymbol{a}_{NS}(f_i, \theta_{n_2})$ is the corresponding near-field steering vector of $s_{n_2}(t)$, so we have

$$\begin{aligned} \boldsymbol{a}_{FS}(f_i, \theta_{n_1}) = [&\exp(-\mathrm{j}2\,\pi f_i \tau_{-M}(\theta_{n_1})), \cdots, \exp(-\mathrm{j}2\,\pi f_i \tau_{-m}(\theta_{n_1})), \cdots, 1, \cdots, \\ &\exp(-\mathrm{j}2\,\pi f_i \tau_m(\theta_{n_1})), \cdots, \exp(-\mathrm{j}2\,\pi f_i \tau_M(\theta_{n_1}))]^{\mathrm{T}} \quad (n_1 = 1, 2, \cdots, N_1) \end{aligned} \quad (4)$$

where

$$\tau_m(\theta_{n_1}) = m\frac{d}{c}\sin\,\theta_{n_1}(m = -M, \cdots, -m, \cdots, 0, \cdots, m, \cdots, M; n_1 = 1, 2, \cdots, N_1) \quad (5)$$

is the propagating delay for the n_1-th $(n_1 = 1, 2, \cdots N_1)$ FFS arriving at the m-th sensor with respect to the reference of the array, similarly

$$\begin{aligned} \boldsymbol{a}_{NS}(f_i, \theta_{n_2}) = {} & [\exp(-\mathrm{j}2\,\pi f_i \tau_{-M}(\theta_{n_2}))\ \cdots, \exp(-\mathrm{j}2\,\pi f_i \tau_{-m}(\theta_{n_2})), \cdots, 1, \cdots, \\ & \exp(-\mathrm{j}2\,\pi f_i \tau_m(\theta_{n_2})), \cdots, \exp(-\mathrm{j}2\,\pi f_i \tau_M(\theta_{n_2}))]^{\mathrm{T}} \quad (n_2 = 1, 2, \cdots, N_2) \end{aligned} \tag{6}$$

Combing geometrical relationship in Fig. 1, we have

$$\tau_m(\theta_{n_2}) = \frac{l_{n_2} - \sqrt{l_{n_2}^2 + (md)^2 - 2l_{n_2} md \sin\theta_{n_2}}}{c} \tag{7}$$

It is the propagating delay for the NFS $s_{n_2}(t)$ arriving at the m-th sensor with respect to the reference of the array, combing Fourier series, we can expand (7) [15]

$$\tau_m(\theta_{n_2}) = -\frac{m^2 d^2}{4l_{n_2} c}\cos 2\theta_{n_2} + \frac{1}{c} md \sin\theta_{n_2} - \frac{m^2 d^2}{4l_{n_2} c} \tag{8}$$

In (1), there is

$$\begin{aligned} \boldsymbol{S}(f_i) &= [\boldsymbol{S}_{FS}(f_i), \boldsymbol{S}_{NS}(f_i)]^{\mathrm{T}} \\ &= [\boldsymbol{S}_1(f_i), \cdots, \boldsymbol{S}_{n_1}(f_i), \cdots, \boldsymbol{S}_{N_1}(f_i), \boldsymbol{S}_{N_1+1}(f_i), \cdots, \boldsymbol{S}_{n_2}(f_i), \cdots, \boldsymbol{S}_N(f_i)]^{\mathrm{T}} \\ &\quad (i = 1, 2, \cdots, J) \end{aligned} \tag{9}$$

it is the signal vector at f_i, where $\boldsymbol{S}_{FS}(f_i) = [\boldsymbol{S}_1(f_i), \cdots, \boldsymbol{S}_{n_1}(f_i), \cdots, \boldsymbol{S}_{N_1}(f_i)]^{\mathrm{T}}$ is the vector of FFS, $\boldsymbol{S}_{NS}(f_i) = [\boldsymbol{S}_{N_1+1}(f_i), \cdots, \boldsymbol{S}_{n_2}(f_i), \cdots, \boldsymbol{S}_N(f_i)]^{\mathrm{T}}$ is that of NFS. $\boldsymbol{E}(f_i)$ is the noise vector with mean 0 and variance $\sigma^2(f_i)$, then the ideal covariance matrix at f_i is

$$\begin{aligned} \boldsymbol{R}(f_i) &= \frac{1}{Z}\boldsymbol{X}(f_i)\boldsymbol{X}^{\mathrm{H}}(f_i) \\ &= \frac{1}{Z}\boldsymbol{A}(f_i, \theta)\boldsymbol{S}(f_i)\boldsymbol{S}^{\mathrm{H}}(f_i)\boldsymbol{A}^{\mathrm{H}}(f_i, \theta) + \sigma^2(f_i)\boldsymbol{I}_{(2M+1)\times(2M+1)} \quad (i = 1, 2, \cdots, J) \\ &= \boldsymbol{R}_{FS}(f_i) + \boldsymbol{R}_{NS}(f_i) + \sigma^2(f_i)\boldsymbol{I}_{(2M+1)\times(2M+1)} \end{aligned} \tag{10}$$

Here the covariance matrix of FFS is $\boldsymbol{R}_{FS}(f_i) = \frac{1}{Z}\boldsymbol{A}_{FS}(f_i)\boldsymbol{S}_{FS}(f_i)\boldsymbol{S}_{FS}^{\mathrm{H}}(f_i)\boldsymbol{A}_{FS}^{\mathrm{H}}(f_i)$, and that of NFS is $\boldsymbol{R}_{NS}(f_i) = \frac{1}{Z}\boldsymbol{A}_{NS}(f_i)\boldsymbol{S}_{NS}(f_i)\boldsymbol{S}_{NS}^{\mathrm{H}}(f_i)\boldsymbol{A}_{NS}^{\mathrm{H}}(f_i)$.

2.2 Array Error Model

When there is gain-phase error in the array, the perturbation at f_i can be expressed by

$$\boldsymbol{W}(f_i) = \mathrm{diag}\Big([W_{-M}(f_i), \cdots, W_{-m}(f_i), \cdots, 1, \cdots, W_m(f_i), \cdots, W_M(f_i)]^{\mathrm{T}}\Big) \quad (i = 1, 2, \cdots, J) \tag{11}$$

where

$$W_m(f_i) = \rho_m(f_i)\mathrm{e}^{\mathrm{j}\phi_m(f_i)}, m = -M, \cdots, -m, \cdots, 0, \cdots, m, \cdots, M \quad (i = 1, 2, \cdots, J) \tag{12}$$

is the gain-phase perturbation of the m-th sensor at f_i, and $\rho_m(f_i)$, $\phi_m(f_i)$ are the gain and phase of the m-th sensor with respect to the 0-th sensor, at the moment, the steering vector of the n-th signal at f_i is

$$\begin{aligned} \boldsymbol{a}'(f_i, \theta_n) &= \begin{bmatrix} W_{-M}(f_i)\mathrm{e}^{-\mathrm{j}2\pi f_i \tau_{-M}(\theta_n)}, \cdots, W_{-m}(f_i)\mathrm{e}^{-\mathrm{j}2\pi f_i \tau_{-m}(\theta_n)}, \cdots, 1, \cdots, \\ W_m(f_i)\mathrm{e}^{-\mathrm{j}2\pi f_i \tau_m(\theta_n)}, \cdots, W_M(f_i)\mathrm{e}^{-\mathrm{j}2\pi f_i \tau_M(\theta_n)} \end{bmatrix}^{\mathrm{T}} \\ &= \mathrm{diag}\Big([W_{-M}(f_i), \cdots, W_{-m}(f_i), \cdots, 1, \cdots, W_m(f_i), \cdots, W_M(f_i)]^{\mathrm{T}}\Big)\boldsymbol{a}(f_i, \theta_n) \\ &= \boldsymbol{W}(f_i)\boldsymbol{a}(f_i, \theta_n) \qquad (n = 1, 2, \cdots, N) \end{aligned} \tag{13}$$

The corresponding array manifold is

$$\begin{aligned} \boldsymbol{A}'(f_i, \theta) &= [\boldsymbol{a}'_{FS}(f_i, \theta_1), \cdots, \boldsymbol{a}'_{FS}(f_i, \theta_{n_1}), \cdots, \boldsymbol{a}'_{FS}(f_i, \theta_{N_1}), \boldsymbol{a}'_{FS}(f_i, \theta_{N_1+1}), \cdots, \boldsymbol{a}'_{FS}(f_i, \theta_{n_2}), \cdots, \boldsymbol{a}'_{FS}(f_i, \theta_N)] \\ &= [\boldsymbol{A}'_{FS}(f_i),\ \boldsymbol{A}'_{FS}(f_i)] \\ &= \boldsymbol{W}(f_i)\boldsymbol{A}(f_i, \theta) \end{aligned} \tag{14}$$

where $\boldsymbol{A}'_{FS}(f_i) = \boldsymbol{W}(f_i)\boldsymbol{A}_{FS}(f_i) = [\boldsymbol{a}'_{FS}(f_i, \theta_1), \cdots, \boldsymbol{a}'_{FS}(f_i, \theta_{n_1}), \cdots, \boldsymbol{a}'_{FS}(f_i, \theta_{N_1})]$ is the array manifold of FFS, $\boldsymbol{a}'_{FS}(f_i, \theta_{n_1})$ is the corresponding steering vector of $s_{n_1}(t)$; $\boldsymbol{A}'_{NS}(f_i) = \boldsymbol{W}(f_i)\boldsymbol{A}_{NS}(f_i) = [\boldsymbol{a}'_{NS}(f_i, \theta_{N_1+1}), \cdots, \boldsymbol{a}'_{NS}(f_i, \theta_{n_2}), \cdots, \boldsymbol{a}'_{NS}(f_i, \theta_N)]$ is the array manifold of NFS, $\boldsymbol{a}'_{NS}(f_i, \theta_{n_2})$ is the corresponding steering vector of $s_{n_2}(t)$, then output of the array at present is

$$\boldsymbol{X}'(f_i) = \boldsymbol{A}'(f_i, \theta)\boldsymbol{S}(f_i) + \boldsymbol{E}(f_i) = \boldsymbol{W}(f_i)\boldsymbol{A}(f_i, \theta)\boldsymbol{S}(f_i) + \boldsymbol{E}(f_i) \quad (i = 1, 2, \cdots, J) \tag{15}$$

For the sake of simplicity, we also define the gain-phase uncertainty vector of the array as

$$\mathbf{w}(f_i) = [\rho_{-M}(f_i)\mathrm{e}^{\mathrm{j}\phi_{-M}(f_i)}, \cdots, \rho_{-m}(f_i)\mathrm{e}^{\mathrm{j}\phi_{-m}(f_i)}, \cdots, 1, \cdots, \rho_m(f_i)\mathrm{e}^{\mathrm{j}\phi_m(f_i)}, \cdots, \rho_M(f_i)\mathrm{e}^{\mathrm{j}\phi_M(f_i)}]^{\mathrm{T}} \tag{16}$$

3 Estimation Theory

First, the covariance matrix at f_i in the presence of gain-phase perturbation is solved by

$$\begin{aligned} \boldsymbol{R}'(f_i) &= \frac{1}{Z}\boldsymbol{X}'(f_i)(\boldsymbol{X}'(f_i))^{\mathrm{H}} \\ &= \frac{1}{Z}\boldsymbol{A}'(f_i,\theta)\boldsymbol{S}(f_i)\boldsymbol{S}^{\mathrm{H}}(f_i)(\boldsymbol{A}'(f_i,\theta))^{\mathrm{H}} + \sigma^2(f_i)\boldsymbol{I}_{(2M+1)\times(2M+1)} \\ &= \frac{1}{Z}\boldsymbol{W}(f_i)\boldsymbol{A}(f_i,\theta)\boldsymbol{S}(f_i)\boldsymbol{S}^{\mathrm{H}}(f_i)\boldsymbol{A}^{\mathrm{H}}(f_i,\theta)\boldsymbol{W}^{\mathrm{H}}(f_i) + \sigma^2(f_i)\boldsymbol{I}_{(2M+1)\times(2M+1)} \\ &= \boldsymbol{R}'_{FS}(f_i) + \boldsymbol{R}'_{NS}(f_i) + \sigma^2(f_i)\boldsymbol{I}_{(2M+1)\times(2M+1)} \end{aligned} \tag{17}$$

Where the covariance matrix of the FFS in the presence of gain-phase perturbation is $\boldsymbol{R}'_{FS}(f_i) = 1/Z \times \boldsymbol{W}(f_i)\boldsymbol{A}_{FS}(f_i)\boldsymbol{S}_{FS}(f_i)\boldsymbol{S}^{\mathrm{H}}_{FS}(f_i)\boldsymbol{A}^{\mathrm{H}}_{FS}(f_i)\boldsymbol{W}^{\mathrm{H}}(f_i)$, that of the NFS is $\boldsymbol{R}'_{NS}(f_i) = 1/Z \times \boldsymbol{W}(f_i)\boldsymbol{A}_{NS}(f_i)\boldsymbol{S}_{NS}(f_i)\boldsymbol{S}^{\mathrm{H}}_{NS}(f_i)\boldsymbol{A}^{\mathrm{H}}_{NS}(f_i)\boldsymbol{W}^{\mathrm{H}}(f_i)$. Eigen-decomposition is performed on $\mathrm{R}'(f_i)$, we can obtain its eigenvector $\boldsymbol{U}'(f_i) = \left[\boldsymbol{U}'_S(f_i)\ \boldsymbol{U}'_E(f_i)\right]$, here $\boldsymbol{U}'_S(f_i)$ is the signal eigenvector and $\boldsymbol{U}'_E(f_i)$ is the noise eigenvector, the former can be utilized to transform the received data on the focusing frequency

$$\boldsymbol{R}''(f_0) = \frac{1}{J}\sum_{i=1}^{J}\boldsymbol{T}(f_i)\boldsymbol{R}'(f_i)\boldsymbol{T}^{\mathrm{H}}(f_i) \tag{18}$$

Where $\boldsymbol{T}(f_i) = \boldsymbol{U}'_S(f_0)\left(\boldsymbol{U}'_S(f_i)\right)^{\mathrm{H}}$ is the focusing matrix, here the center frequency can be used as f_0. Similarly, Eigen-decomposition is performed on $\boldsymbol{R}''(f_0)$, its noise eigenvector $\boldsymbol{U}_E(f_0)$ is obtained, then combining multiple signal classification algorithm, we can establish the following spatial spectrum

$$\begin{aligned} P_{MU-F}(\theta) &= \frac{1}{(\boldsymbol{a}'_{FS}(f_0,\theta))^{\mathrm{H}}\boldsymbol{U}_E(f_0)\boldsymbol{U}^{\mathrm{H}}_E(f_0)\boldsymbol{a}'_{FS}(f_0,\theta)} \\ &= \frac{1}{\boldsymbol{a}^{\mathrm{H}}_{FS}(f_0,\theta)\boldsymbol{W}^{\mathrm{H}}(f_0)\boldsymbol{U}_E(f_0)\boldsymbol{U}^{\mathrm{H}}_E(f_0)\boldsymbol{W}(f_0)\boldsymbol{a}_{FS}(f_0,\theta)} \\ &= \frac{1}{Y} \end{aligned} \tag{19}$$

Perform the following transformation on the denominator of the function above

$$Y = \sum_{n_1=1}^{N_1}\boldsymbol{a}^{\mathrm{H}}_{FS}(f_0,\theta_{n_1})\boldsymbol{W}^{\mathrm{H}}(f_0)\boldsymbol{U}_E(f_0)\boldsymbol{U}^{\mathrm{H}}_E(f_0)\boldsymbol{W}(f_0)\boldsymbol{a}_{FS}(f_0,\theta_{n_1}) \tag{20}$$

Simplify (20), we have

$$\begin{aligned} Y &= \sum_{n_1=1}^{N_1} \boldsymbol{a}_{FS}^{\mathrm{H}}(f_0,\theta_{n_1})\boldsymbol{W}^{\mathrm{H}}(f_0)\boldsymbol{U}_E(f_0)\boldsymbol{U}_E^{\mathrm{H}}(f_0)\boldsymbol{W}(f_0)\boldsymbol{a}_{FS}(f_0,\theta_{n_1}) \\ &= \sum_{n_1=1}^{N_1} \boldsymbol{w}^{\mathrm{H}}(f_0)\left\{ (\mathrm{diag}(\boldsymbol{a}_{FS}(f_0,\theta_{n_1})))^{\mathrm{H}}\boldsymbol{U}_E(f_0)\boldsymbol{U}_E^{\mathrm{H}}(f_0)\mathrm{diag}(\boldsymbol{a}_{FS}(f_0,\theta_{n_1})) \right\}\boldsymbol{w}(f_0) \\ &= \boldsymbol{w}^{\mathrm{H}}(f_0)\boldsymbol{D}(f_0,\theta)\boldsymbol{w}(f_0) \end{aligned} \tag{21}$$

Where $\boldsymbol{D}(f_0,\theta) = \sum_{n_1=1}^{N_1}\left\{(\mathrm{diag}(\boldsymbol{a}_{FS}(f_0,\theta_{n_1})))^{\mathrm{H}}\boldsymbol{U}_E(f_0)\boldsymbol{U}_E^{\mathrm{H}}(f_0)\mathrm{diag}(\boldsymbol{a}_{FS}(f_0,\theta_{n_1}))\right\}$, the DOA of FFS can be solved by minimizing (21). As $\boldsymbol{w}(f_0) \neq \boldsymbol{0}$, $\boldsymbol{w}^{\mathrm{H}}(f_0)\boldsymbol{D}(f_i,\theta)\boldsymbol{w}(f_0)$ will equal zero only if $\boldsymbol{D}(f_0,\theta)$ is singular, then θ corresponds to the actual DOA at the moment, so $\theta_1,\cdots\theta_{N_1}$ can be estimated by solving N_1 roots of the following polynomial

$$|\boldsymbol{D}(f_0,\theta)| = 0 \tag{22}$$

The proposed method is suitable for far-field sources in mixed wideband signals, so we can call it FMW method.

4 Simulations

Here, some simulations are presented for the method, consider some wideband chirp signals impinge on a uniform linear array with 11 omnidirectional sensors, the sixth sensor is defined as the reference, three FFS and two NFS arriving at the array from $(25°, 35°, 45°)$ and $(5°, 15°)$ synchronously. The frequency of these wideband signals is limited in $[0.1\ \text{GHz}, 0.12\ \text{GHz}]$, and spacing d between adjacent sensors is equal to half of the wavelength of the center frequency, the signal band is divided into 30 bins. Here we will simplify the generation of the error, so the gain and phase of the every sensor relative to the reference are respectively selected in $[0, 1.6]$ and $[-24°, 24°]$, the average of 200 Monte-Carlo trials is regarded as the result. EGP [10], MFN [16], two-sided correlation transformation (TCT) [17] and FMW are respectively utilized for the estimation.

4.1 DOA Estimation for Narrowband Signals

Figure 2 is the estimation errors versus SNR at 0.11 GHz when sampling times Z is 20; Fig. 3 presents that versus sampling times Z at 0.11 GHz when SNR is 6 dB. It can be seen from Figs. 2 and 3, estimation errors decrease with the increase of SNR or sampling times, and they are convergent finally. MFN can not apply to the gain-phase perturbation, even though SNR is high or sampling times is large, a large error can not be avoided all the same; EGP has to calibrate the array before estimating FFS, which will also bring some uncertainty; By contrast, FMW is not necessary to correct the array before calculating FFS, so it performs better than the other two methods.

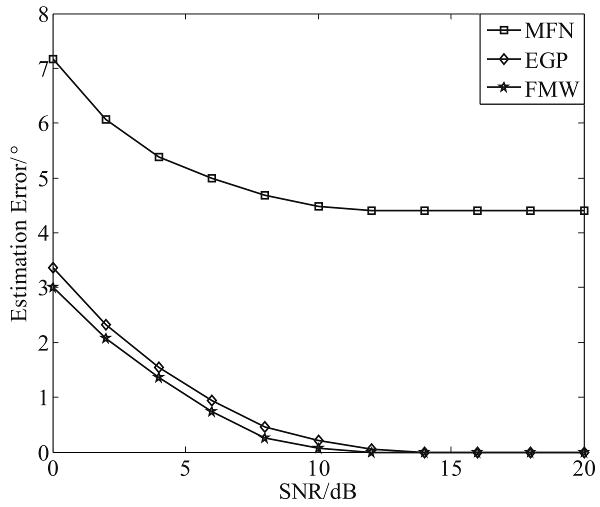

Fig. 2. DOA estimation errors at 0.11 GHz versus SNR

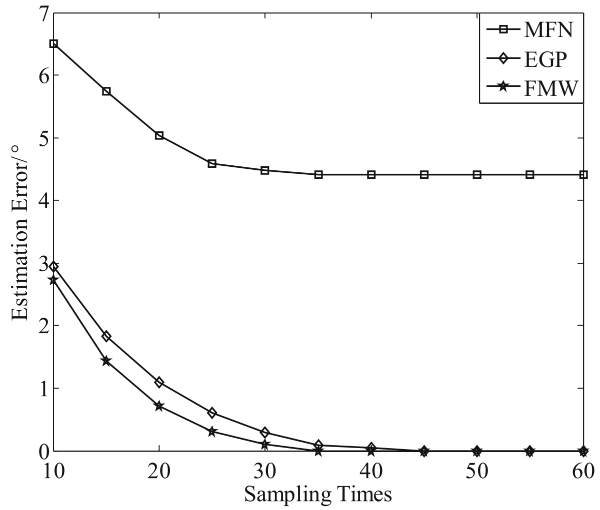

Fig. 3. DOA estimation errors at 0.11 GHz versus sampling times

4.2 DOA Estimation for Wideband Signals

Figure 4 shows estimation error versus SNR of wideband coherent signals when sampling times Z is 20; and Fig. 5 verifies that versus sampling times Z of wideband coherent signals when SNR is 6 dB.

From Figs. 4 and 5 we know that FMW is still effective to wideband coherent signals by focusing, and there are no obvious differences comparing with the circumstance of narrowband signals; though TCT is also suitable for wideband signals, it has failed owing to the array error.

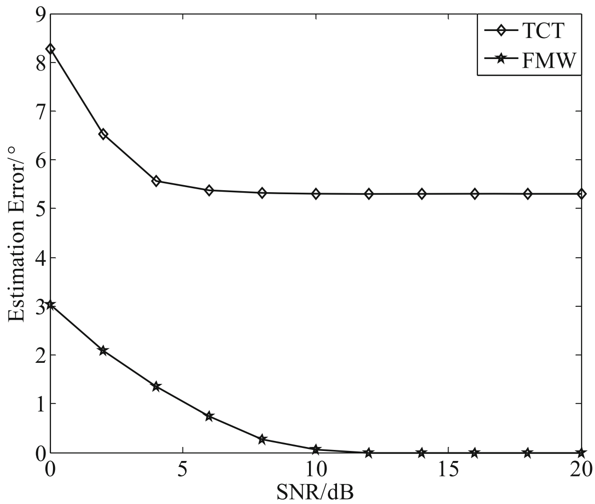

Fig. 4. DOA estimation errors of wideband coherent signals versus SNR

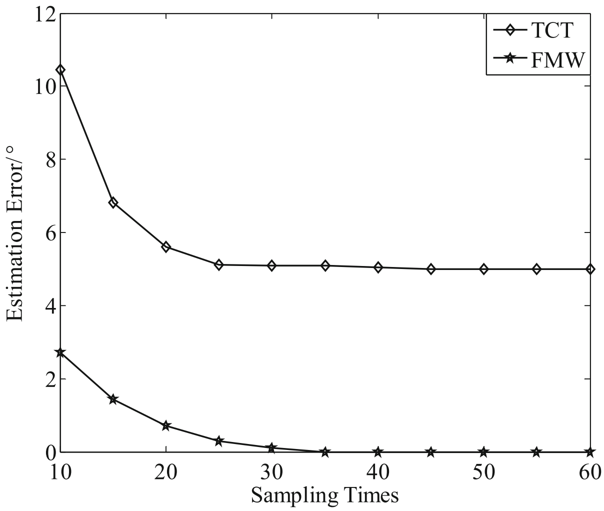

Fig. 5. DOA estimation errors of wideband coherent signals versus sampling times

5 Conclusion

In the paper, a new method of estimating DOA of FFS in mixed FFS and NFS with gain-phase error array is provided. It both applies to narrowband and wideband coherent signals. In the meantime, it averts spectrum searching by directly finding roots of the polynomial according to the special structure of the array, so the computational efficiency is improved to a great extent.

Acknowledgments. I would like to thank Heilongjiang province ordinary college electronic engineering laboratory and post doctoral mobile stations of Heilongjiang University.

References

1. Otte, W.R., Gokhale, A., Schmidt, D.C.: Efficient and deterministic application deployment in component-based enterprise distributed real-time and embedded systems. Inf. Softw. Technol. **55**, 475–488 (2013)
2. Shafiq, M., Hussain, G.A.: Partial discharge diagnostic system for smart distribution networks using directionally calibrated induction sensors. Electr. Power Syst. Res. **119**, 447–461 (2015)
3. Yusuke, H., Jihoon, H., Tomoaki, O.: Activity recognition using array antenna. In: 2015 IEEE International Conference on Communications, pp. 507–511. IEEE Press, Hangzhou (2015)
4. Sanchez, L., Munoz, L., Galache, J.A.: SmartSantander: IoT experimentation over a smart city testbed. Comput. Netw. **61**, 217–238 (2014)
5. Han, G., Wan, L., Shu, L., Feng, N.: Two novel DOA estimation approaches for real-time assistant calibration systems in future vehicle industrial. IEEE Syst. J. **99**, 1–12 (2015)
6. Li, J., Zhao, Y.J., Li, D.H.: Accurate single-observer passive coherent location estimation based on TDOA and DOA. Chin. J. Aeronaut. **27**, 913–923 (2014)
7. Fabrizio, G., Heitmann, A.: A multipath-driven approach to HF geolocation. Sig. Process. **93**, 3487–3503 (2013)
8. Lee, J., Chen, Y., Yeh, C.: A covariance approximation method for near-field direction finding using a uniform linear array. IEEE Trans. Sig. Process. **43**, 1293–1298 (1995)
9. Liu, A.F., Liao, G.S., Zeng, C.: An eigenstructure method for estimating DOA and sensor gain-phase errors. IEEE Trans. Sig. Process. **59**, 5944–5956 (2011)
10. Cao, S.H., Ye, Z.F., Hu, N.: DOA estimation based on fourth-order cumulants in the presence of sensor gain-phase errors. Sig. Process. **93**, 2581–2585 (2013)
11. Han, K.Y., Yang, P., Nehorai, A.: Calibrating nested sensor arrays with model errors. IEEE Trans. Antennas Propag. **63**, 4739–4748 (2015)
12. Liang, J.L., Liu, D.: Passive localization of mixed near-field and far-field sources using two-stage MUSIC algorithm. IEEE Trans. Sig. Process. **58**, 108–120 (2010)
13. Wang, K., Wang, L., Shang, J.R.: Mixed near-field and far-field source localization based on uniform linear array partition. IEEE Sens. J. **16**, 8083–8090 (2016)
14. Ye, T., Sun, X.Y.: Mixed sources localisation using a sparse representation of cumulant vectors. IET Sig. Process. **8**, 606–611 (2014)
15. Vleck, E.B.V.: The influence of Fourier's serious upon the development of mathematics. Science **39**, 113–124 (1914)
16. He, J., Swamy, M.N.S., Ahmad, M.O.: Efficient application of MUSIC algorithm under the coexistence of far-field and near-field sources. IEEE Trans. Sig. Process. **60**, 2066–2070 (2012)
17. Valaee, S., Kabal, P.: Wideband array processing using a two-sided correlation transformation. IEEE Trans. Sig. Process. **43**, 160–172 (1995)